Syntheses, Characterization, Antimicrobial and DNA Cleavage Activity of Cr(III) Complexes with Coumarin based Schiff Base Ligands

Ramhari Meena[iD], Anita Kumari[iD], Naveen Sharma[iD] and Nighat Fahmi[*,iD]

Department of Chemistry, University of Rajasthan, Jaipur-302004, India

*Corresponding author: E-mail: ramharichem@gmail.com; nighat.fahmi@gmail.com

A series of biologically important complexes of chromium(III) have been synthesized by the reaction of 3-formyl-4-chlorocoumarin hydrazinecarbothioamide (L^1H) and 3-formyl-4-chlorocoumarin hydrazinecarboxamide (L^2H) with $CrCl_3 \cdot 6H_2O$ in 1:1 and 1:2 molar ratio. All the complexes have been characterized by elemental analysis, molecular weight determination, melting point, conductivity measurements, electronic, IR, ^1H NMR, ^{13}C NMR and EPR spectroscopic techniques and X-ray diffraction. *In vitro* biological screening effects of the compounds were tested against the pathogenic bacterial and fungal species. Further, free ligands and their metal complexes have been screened for their DNA cleavage activity. A comparative study of the biological activities of the Schiff base ligands and their Cr(III) complexes indicates that the complexes exhibit higher antimicrobial and DNA cleavage activity than the free ligands. Physico-chemical studies and spectral data suggested a hexa-coordinated environment around the central metal ion.

Keywords: Coumarin, Schiff base ligands, Cr(III) complexes, Antimicrobial activity, DNA cleavage activity.

INTRODUCTION

In humans, trivalent chromium(III) has a favourable role in managing sugar and lipid metabolism in trace amounts [1], and its shortage is thought to cause chromium deficiency. Only a little amount of chromium(III) enters the cells due to unique transport systems. High amounts of chromium(III) in the cell have been shown to cause DNA damage in various *in vitro* investigations. Recent reviews imply that moderate intake of chromium(III) through dietary supplements causes little harm [2]. Chromium compounds were utilized in dyes and paints, as well as in leather tanning. Because chromium exhibits varied oxidation states, spin states, coordination numbers, and redox characteristics in different chromium complexes, it is an essential metal for catalytic studies [3].

Researchers are becoming increasingly interested in coordination compounds as a result of its crucial applications in the field of biological probes [4]. Because of their biological activity, such as antitumor, antibacterial, fungicidal and anticarcinogenic capabilities, a vast variety of Schiff bases and their complexes are of great interest. Antimicrobial, anticoagulant and plant growth regulating actions are all demonstrated by coumarin-based Schiff bases and their metal complexes [5-8]. Biological activity of chromium(III) coordination compounds with Schiff base ligands include antibacterial, antifertility, pesticidal and nematicidal properties [9-12]. Herein, we report the synthesis and characterization of chromium(III) complexes $[Cr(L^1)Cl_2(H_2O)_2]$ (**1**), $[Cr(L^1)_2Cl(H_2O)]$ (**2**), $[Cr(L^2)Cl_2(H_2O)_2]$ (**3**) and $[Cr(L^2)_2Cl(H_2O)]$ (**4**) derived from bidentate ligands 3-formyl-4-chlorocoumarin hydrazinecarbothioamide (L^1H) and 3-formyl-4-chlorocoumarin hydrazinecarboxamide(L^2H), respectively having N∩S and N∩O donor atom. The *in vitro* biological activity of the compounds was assessed against various bacteria (*Pseudomonas aeruginosa* and *Streptococcus pyogenes*) and fungi (*Candida albicans* and *Fusarium semitectum*). Further, these complexes were also tested for DNA cleavage activity and the results were indeed positive.

EXPERIMENTAL

All of the chemicals and solvents utilized were of A.R. grade. Analytical grade 4-hydroxycoumarin was purchased from Sigma-Aldrich. Merck provided the highest purity of the analytical grade metal salt, which was used exactly as received. All of the solvents used were of standard quality.
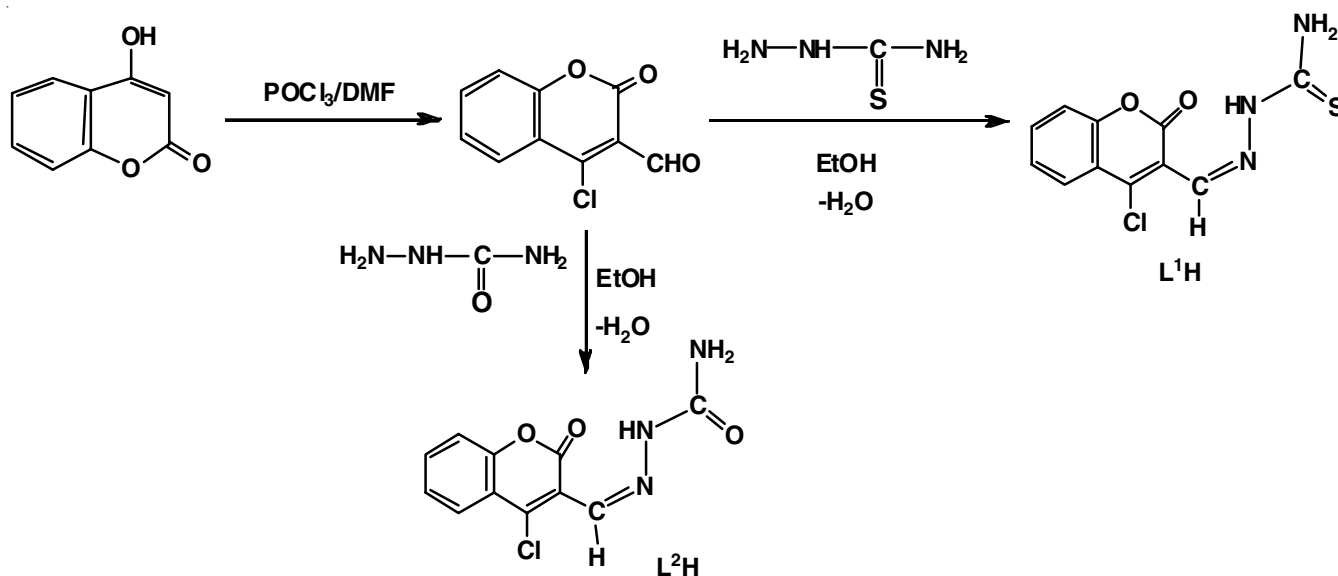
Open capillaries were used in the electric melting point device to determine the melting point. The century digital conductivity meter type CC 601 was used to measure the conductivity. At RSIC, IIT Madras, Chennai, India, the electronic spectra were recorded on a Varian-Cary/2390 spectrophotometer. In DMSO-d_6, spectra of ^{1}H and ^{13}C NMR were collected using TMS as the internal standard on a Bruker Avance-III 400 MHz FT NMR spectrometer. On a Nicolet Megna FTIR-550 spectrophotometer, KBr pellets were used to record infrared spectra. At SAIF, IIT Madras, Chennai, India, the complexes' EPR spectra were monitored using a Varian E-4X band spectrometer.

Synthesis of 3-formyl-4-chlorocoumarin: 3-Formyl-4-chlorocoumarin was prepared by the formylation of 4-hydroxycoumarin as reported [13]. Phosphorus oxychloride (10 mL) was added dropwise to a dimethylformamide (20 mL) solution while keeping the temperature below 5 ℃. After that a solution of 4-hydroxycoumarin (4.0 g) in DMF (10 mL) was progressively added to the mixture, while it was constantly stirred and the temperature was kept below 5 ° C. The reaction mixture was then left at room temperature for 2 h before being heated in a steam bath for 1 h. After cooling, the reaction mixture was poured onto crushed ice and neutralized with sodium carbonate (**Scheme-I**). A solid product was immediately formed and crystallized from ethanol to give a yellow solid (m.p. 115 ℃, yield: 3.2 g; 80%).
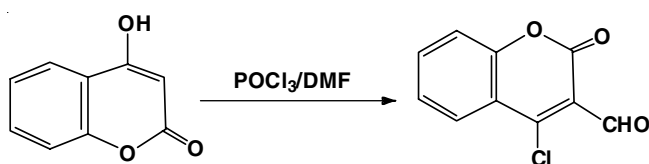
Scheme-I: Synthetic scheme of the 3-formyl-4-chlorocoumarin

Synthesis of ligands (L^{1}H and L^{2}H): Two ligands, 3-formyl-4-chlorocoumarin hydrazinecarbothioamide (L^{1}H) and 3-formyl-4-chlorocoumarin hydrazinecarboxamide (L^{2}H), were prepared by reacting 3-formyl-4-chlorocoumarin (2.68 g, 0.01 mol) with thiosemicabazide (1.55 g, 0.01 mol) (in presence of sodium acetate) and semicarbazide hydrochloride (1.90 g, 0.01 mol) in 1:1 molar ratio in 100 mL ethanol as solvent, respectively. The reactions were completed in 3-4 h (**Scheme-II**). The solution was then concentrated under reduced pressure, yielding crystalline precipitates after cooling. The products were dried after being washed and recrystallized in the same solvent. The yields of the ligands L^{1}H and L^{2}H were 77% and 72 %, respectively.

Synthesis of Cr(III) complexes

Synthesis of [Cr(L^1)Cl$_2$(H$_2$O)$_2$] and [Cr(L^2)Cl$_2$(H^{2}O)$_2$] complexes: To CrCl$_3$·6H$_2$O (2.65 g, 0.01 mol) dissolved in dry methanol and methanolic solution of ligands (L^{1}H, 2.81 g, 0.01 mol and L^{2}H, 2.65 g, 0.01 mol) was added separately in 1:1 molar ratio using NaOH in appropriate stoichiometric proportions. The resulting mixture was heated under reflux for 14-16 h, filtered to remove NaCl and the solvent was concentrated under reduced pressure. The product was dried in a vacuum. The resulting compounds were washed with cyclohexane and recrystallized with methanol. The green crystals were dried under a vacuum for few hours to give a yield of 71%.

Synthesis of [Cr(L^1)$_2$Cl(H$_2$O)] and [Cr(L^2)$_2$Cl(H$_2$O)] complexes: The complexes were prepared by reaction of CrCl$_3$·6H$_2$O (1.32 g, 0.005 mol) and the respective ligands (L^{1}H (2.81 g, 0.01 mol) and L^{2}H (2.65 g, 0.01 mol) in 1:2 molar ratio using appropriate stoichiometric proportions in dry methanol in the presence of NaOH. The resulting mixture was heated under reflux for 14-17 h, filtered to remove NaCl and the solvent was concentrated under reduced pressure. The product was dried in vacuum. The resulting compounds were washed with cyclohexane and recrystallized with methanol. The green crystals were dried under a vacuum for few hours to give a yield of 77%. Elemental analyses were conducted using the standard methods and their results were found to be in good agreement with the calculated values (Table-1).

Scheme-II: Synthetic scheme of the ligands

TABLE-1
ANALYTICAL DATA AND PHYSICAL PROPERTIES OF THE LIGANDS AND THEIR Cr(III) COMPLEXES

Compounds	Colour	m.p. (°C)	Elemental analysis (%): Found (calcd.)						m.w. found (calcd.)
			C	H	N	S	Cl	M	
L^{1}H	Yellow	127	46.02 (46.90)	2.61 (2.86)	14.16 (14.92)	10.98 (11.38)	12.03 (12.58)	–	280.54 (281.72)
L^{2}H	White	133	49.60 (49.73)	2.98 (3.04)	15.55 (15.82)	–	13.24 (13.35)	–	264.35 (265.65)
[CrCl$_2$(L^1)(H$_2$O)$_2$]	Yellow	205-208(d)	29.72 (30.05)	2.07 (2.52)	9.10 (9.56)	6.81 (7.29)	23.88 (24.19)	11.49 (11.83)	438.19 (439.64)
[CrCl(L^1)$_2$(H$_2$O)]	Yellow	203-204(d)	38.25 (39.62)	2.09 (2.42)	12.26 (12.60)	9.21 (9.62)	15.53 (15.95)	7.46 (7.80)	665.47 (666.88)
[CrCl$_2$(L^2)(H$_2$O)$_2$]	Green	203-205(d)	30.76 (31.19)	2.23 (2.62)	9.58 (9.92)	–	24.89 (25.11)	11.85 (12.28)	422.12 (423.58)
[CrCl(L^2)$_2$(H$_2$O)]	Green	199-202(d)	41.25 (41.63)	2.16 (2.54)	12.94 (13.24)	–	16.39 (16.76)	7.81 (8.19)	633.27 (634.75)

Antibacterial activity: The agar disc diffusion method was used for an *in vitro* antibacterial study [14]. *Pseudomonas aeruginosa* and *Streptococcus pyogenes* were the bacterial species used in the screening. Each compound was dissolved in methanol and concentration solutions (500 and 1000 ppm) were made separately. Paper discs of uniform diameter (5 mm) of Whatman filter paper (no. 1) were cut and sterilized in an autoclave. The paper discs were placed aseptically in petri plates containing nutritional agar media (agar 20 g + beef extract 3 g + peptone 5 g) seeded with *Pseudomonas aeruginosa* and *Streptococcus pyogenes* separately. The petri dishes were incubated at 37 ºC for 24 h and the inhibition zones were measured. Using the same method, the antibacterial activity of the standard antibiotic streptomycin was also measured. The percent activity index was determined using the following formula:

$$\text{Activity index (\%)} = \frac{\text{Zone of inhibition by test compound (diameter)}}{\text{Zone of inhibition by standard (diameter)}} \times 100$$

Antifungal activity: Agar plate technique [14] was used to assess the antifungal activity of the produced compounds against the two pathogenic fungus *Candida albicans* and *Fusarium semitectum*. To keep the fungal growth going, a potato dextrose agar (PDA) medium was created in the lab. PDA was prepared by extracting 20 g potato with distilled water (100 mL) at 100 ºC for 1 h and filtering it with a cotton filter. Then, the potato juice was mixed with 2 g dextrose, 1.5 g agar and the pH of the resulting PDA media was adjusted to 7. The test chemicals were dissolved in methanol at the concentrations of 100 and 200 ppm before being combined with the medium. The media was then poured into petri plates and fungus spores were deposited on top of the medium using an inoculum needle. These petri plates were placed in an incubator at 25 ± 2 ºC after being covered in polythene bags containing a few drops of alcohol. After 96 h of incubation at room temperature (25 ºC), the activity was measured. Controls were also done, with three replicates in each case. The linear growth of the fungus was determined by measuring the diameter of the fungal colony in petri plates after four days. The outcomes were compared to the conventional fungicide (itraconozole).

The percentage inhibition was calculated as:

$$\text{Inhibition (\%)} = \frac{C - T}{C} \times 100$$

where, C and T are the diameters of the fungus colony in the control and test plates, respectively.

DNA cleavage study

Primary culture of *E. coli*: About 24 h old culture of *E. coli* growing on nutritional broth (peptone 5 g, beef extract 3 g, sodium chloride 5 g, distilled water 1000 mL, pH 7.0 autoclaved at 121 ºC, 15 psi pressure and 15 min). The ATCC 25922 *E. coli* culture was added to the media. To obtain secondary culture, the original culture was moved to fresh nutrient broth (25 mL primary culture and 25 mL fresh medium).
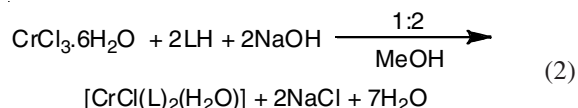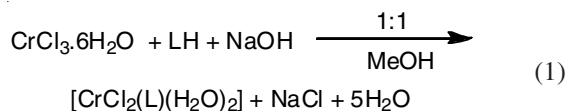
Isolation of genomic DNA: The following approach was used to isolate the DNA. The pellet was obtained by centrifuging 1.5 mL of fresh bacterial culture. This was done by dissolving the pellet in 0.5 mL lysis buffer (100 mmol L^{-1} tris pH 8.0, 50 mmol L^{-1} EDTA, 50 mmol L^{-1} lysozyme). Incubation at 55 ºC for 10 min was followed by centrifugation at 10,000 rpm for 10 min. It was then centrifuged at 10,000 rpm for 10 min with an equal amount of chloroform-isoamyl alcohol (24:1) and 1/20th volume of 3 mol L^{-1} sodium acetate (pH 4.8) before adding three volumes of cold absolute alcohol. Centrifugation was used to separate the DNA precipitate. Using a TAE buffer (100 mmol L^{-1} tris pH 8.0 adjusted with glacial acetic acid, 10 mmol L^{-1} EDTA) and storing it in the freezer, the pellet was dried and dissolved.

Treatment of DNA with samples: Separately, compounds (500 ppm) were added to the DNA sample and incubated for 2 h at 37 ºC.

Agarose gel electrophoresis: Following the treatment of DNA samples, the samples were electrophoresed using the following process. By boiling, 200 mg of agarose were dissolved in 25 mL of TAE buffer (4.84 g Tris base, pH 8.0, 0.5 mol L^{-1} EDTA/1 L). When the gel reached 5 ºC, it was placed into a comb-equipped gel cassette. The gel had hardened. The comb was gently removed and the gel was placed in a TAE buffer-flooded electrophoresis chamber. A total of 20 mL of DNA sample (combined in a 1:1 ratio with bromophenol blue dye) was carefully placed into the wells, along with a control and a constant 50 V of electricity was passed for 30 min. The gel was carefully removed, stained for 10-15 min with ethidium bromide solution (10 mg mL^{-1}) and the bands were examined using a UV transilluminator.

RESULTS AND DISCUSSION

Elemental analysis and spectral data of Cr(III) complexes exhibited 1:1 and 1:2 metal-ligand stoichiometry of the types $[Cr(L^1)Cl_2(H_2O)_2]$, $[Cr(L^2)Cl_2(H_2O)_2]$ and $[Cr(L^1)_2Cl(H_2O)]$, $[Cr(L^2)_2Cl(H_2O)]$, where L^1 and L^2 work together as a bidentate ligand. Their monomeric nature is shown by their molecular weights determinations. The creation of these complexes can be based on the following eqns. 1 and 2:

$$CrCl_3 \cdot 6H_2O + LH + NaOH \xrightarrow[\text{MeOH}]{1:1}$$
$$[CrCl_2(L)(H_2O)_2] + NaCl + 5H_2O \quad (1)$$

$$CrCl_3 \cdot 6H_2O + 2LH + 2NaOH \xrightarrow[\text{MeOH}]{1:2}$$
$$[CrCl(L)_2(H_2O)] + 2NaCl + 7H_2O \quad (2)$$

Metal complexes dissolve in DMSO, MeOH and DMF. At 25 ºC, the molar conductivities of 10^{-3} M Cr(III) complexes solution were measured. Molar conductance values for complexes have been reported to be in the range of 5-26 ohm^{-1} cm^{-2} mol^{-1} indicating that they are non-electrolytic in nature.

Electronic spectra: In methanol, the electronic spectra of Schiff base ligands (L^1H-L^2H) as well as their chromium(III) complexes were recorded. The broad band at 26315-27247 cm^{-1} in the electronic spectra of the ligands can be attributed to the azomethine group's n-π* transitions, which undergo a blue shift upon complexation due to nitrogen atom binding to the central metal atom. The nitrogen in the azomethine group of the ligand donates a lone pair of electrons to the central metal ion, causing this shift. The electronic spectra of Cr(III) complexes showed three bands at 16456-17413, 22880-24138 and 30221-32486 cm^{-1}, which correspond to the $^4A_{2g} \rightarrow {}^4T_{2g}(\nu_1)$,

$^4A_{2g} \rightarrow {}^4T_{1g}(\nu_2)$ and $^4A_{2g} \rightarrow {}^4T_{1g}(P)(\nu_3)$ *d-d* transitions, respectively. The octahedral geometry of the Cr^{3+} ion is suggested by these three transitions. Table-2 summarizes the results of several ligand field parameters such as Dq, B and β. The energy of the first spin-allowed transition [$^4A_{2g}$ (F) - $^4T_{2g}$ (F)] directly gives the value of 10Dq. The Rach parameter is used to express the electronic repulsion parameter and 'B' is evaluated in these investigations. The results are on the order of 56-65% of the free ion value, indicating a significant amount of orbital overlap. Newly synthesized Cr(III) complexes have β values in the range of 0.69 to 0.71, which are similar to Cr(III) complexes described earlier in the literature [15]. The nephelauxetic ratio suggests that the complexes are significantly covalent in nature.

IR spectra: Table-3 lists the diagnostic IR spectral bands of the ligands and their complexes, as well as their preliminary assignments. The free ligands' IR spectra (L^1H and L^2H) show bands about *ca.* 1635-1630 cm^{-1}, which are assigned to ν(>C=N). Because of the coordination of the imine nitrogen to the metal ion, the bands in the IR spectra of the complexes due to ν(>C=N) moved to a lower frequency. The free ligands' IR spectra display a medium intensity band at 3240-3155 cm^{-1} due to ν(N-H), which is absent in the complexes' spectra. The L^1H and L^2H IR spectra show two sharp bands about 3485-3340 and 3500-3350 cm^{-1}, which correspond to NH$_2$ group ν_{sym} and ν_{asym} vibrations, respectively. These bands are unaffected by the Cr(III) complexes, showing that the NH$_2$ group is not involved in coordination. The ligands (L^1H)/(L^2H) display a band at the ν(C=S)/(C=O) stretching frequency of 1080/1715 cm^{-1}. The >C=S/>C=O band appears weak in the complexes and is shifted to a lower wave number, demonstrating the coordination nature of the M-S/M-O bond. In Cr(III) complexes, the band at 1735 cm^{-1} caused by (>C=O of lactone) remains unaltered,

TABLE-2
ELECTRONIC SPECTRAL DATA (cm^{-1}) OF THE CHROMIUM(III) COMPLEXES

Compounds	Transitions	Spectral bands (cm^{-1})	Dq	B	β = B/B°	ν_2/ν_1
$[CrCl_2(L^1)(H_2O)_2]$	$^4A_{2g}$ (F) → $^4T_{2g}$(F) $^4A_{2g}$(F) → $^4T_{1g}$(F) $^4A_{2g}$(F) → $^4T_{1g}$(P)	16456 22880 31372	1645	637	0.69	1.39
$[CrCl(L^1)_2 (H_2O)]$	$^4A_{2g}$ (F) → $^4T_{2g}$(F) $^4A_{2g}$(F) → $^4T_{1g}$(F) $^4A_{2g}$(F) → $^4T_{1g}$(P)	17381 23852 32010	1738	633	0.68	1.37
$[CrCl_2(L^2)(H_2O)_2]$	$^4A_{2g}$ (F) → $^4T_{2g}$(F) $^4A_{2g}$(F) → $^4T_{1g}$(F) $^4A_{2g}$(F) → $^4T_{1g}$(P)	16935 23629 32486	1693	666	0.72	1.39
$[CrCl(L^2)_2 (H_2O)]$	$^4A_{2g}$ (F) → $^4T_{2g}$(F) $^4A_{2g}$(F) → $^4T_{1g}$(F) $^4A_{2g}$(F) → $^4T_{1g}$(P)	17413 24138 30221	1741	665	0.71	1.38

TABLE-3
IR (cm^{-1}) SPECTRAL DATA OF THE LIGANDS AND THEIR METAL COMPLEXES

Compound	ν(NH)	ν(OH)	ν(C=N)	ν(M-O)	ν(M←N)
L^1H	3240	–	1630	–	–
L^2H	3155	–	1635	–	–
$[CrCl_2(L^1)(H_2O)_2]$	–	3458	1612	–	446
$[CrCl(L^1)_2(H_2O)]$	–	3460	1615	–	430
$[CrCl_2(L^2)(H_2O)_2]$	–	3455	1610	605	435
$[CrCl(L^2)_2(H_2O)]$	–	3470	1617	590	420

TABLE-4								
X-RAY POWDER DIFFRACTION DATA OF $[CrCl(L^1)_2(H_2O)]$								
h	k	l	2θ (Exp.)	2θ (Calc.)	2θ (Diff.)	d (Exp.)	d (Calc.)	Intensity (Exp.)
0	0	2	15.02	15.52	-0.5	6.3863	6.3685	11.45
3	0	1	26.72	26.37	-0.35	3.8411	3.8364	8.12
3	0	3	27.21	27.93	-0.72	2.9862	2.9203	11.25
3	1	2	28.12	28.45	-0.33	2.9681	2.9166	91.23
4	0	3	43.92	44.60	-0.68	2.4933	2.4595	7.21

showing that the lactone oxygen is not engaged in coordination. A band in the region of 880-876 cm^{-1} may be seen in the spectra of all Cr(III) complexes, which could be attributable to the coordinated water molecule. Furthermore, the broadband at 3455-3470 cm^{-1} could be due to the water molecules ν(O-H). Non-ligand bands attributable to ν(Cr–N) and ν(Cr–O) in the spectra of chromium(III) complexes around 446-420 and 600-590 cm^{-1}, respectively, further support the ligands' complexation to the metal ion.

^{1}H & ^{13}C NMR spectra: ^{1}H & ^{13}C NMR spectra of both ligands (L^{1}H) and (L^{2}H), corroborated their structure. The signal peak due to –NH– protons revealed a prominent and sharp peak at 8.70-9.05 ppm in the ^{1}H NMR spectra of the ligands recorded in DMSO-d_6. The ligands (L^{1}H) and (L^{2}H) have peaks of –NH$_2$ protons at 3.45 and 3.65 ppm, respectively. At 6.72 ppm, a substantial azomethine proton signal attributable to -CH=N was detected, while aromatic protons were detected in the range of 6.70-8.10 ppm. The signal owing to the azomethine carbon atom of the ligands emerges at 166.50-169.30 ppm in ^{13}C NMR data for both the ligands. Carbons connected to the thiolic and enolic oxygen give rise to signals at 162.80 and 175.70 ppm, respectively.

X-ray powder diffraction study: Based on X-ray powder diffraction studies, the potential lattice dynamics of the finely powdered chromium(III) complex $[CrCl(L^1)_2(H_2O)]$ have been determined. The observed interplanar spacing values (d) were calculated from the diffractogram of the compound $[CrCl(L^1)_2(H_2O)]$ and the Miller indices *h*, *k* and *l* were assigned to each d value, with 2θ angles reported in Table-4. The results demonstrated that the chemical conforms to the 'orthorhombic' crystal system, with unit cell characteristics of a = 9.1000, b = 17.3000, c = 21.0100, maximum deviation of 2θ = 0.2° and α = 90°, β = 90°, γ = 90° at the wavelength = 1.54 Å.

EPR spectra and magnetic moments: At ambient temperature, the EPR spectra were captured as a polycrystalline sample. The extent of unpaired electron delocalization is determined by the ESR spectra of Cr(III) complexes. The newly synthesized Cr(III) complexes consist a single broad peak. Table-5 shows the results of the ESR parameters and the Lande splitting factor (g values). The 'g' value of the present complexes was found to be in the range of 1.9616-1.9858 in ESR spectra and 'g' values are closer to g_{iso} (g_{iso} = 2), implying an octahedral geometry. At room temperature, the magnetic moments of the Cr(III) complexes are 3.67-3.82 B.M., equivalent to three unpaired electrons.

The complexes may be tentatively recommended to have octahedral geometry and proposed 3D-structures of the Cr(III) complexes based on the physico-chemical and spectral data

Compound	H$_0$	g value	Temp. (°C)	Megetic moment (μ)
TABLE-5				
ESR SPECTRAL DATA OF THE CHROMIUM(III) COMPLEXES				
$[CrCl_2(L^1)(H_2O)_2]$	3300.25	1.9706	25	3.73
$[CrCl(L^1)_2(H_2O)]$	3315.35	1.9616	25	3.82
$[CrCl_2(L^2)(H_2O)_2]$	3275.20	1.9858	25	3.67
$[CrCl(L^2)_2(H_2O)]$	3315.26	1.9618	25	3.79

presented and discussed above (Fig. 1). Due to the existence of three unpaired electrons in Cr(III) complexes, magnetic investigations of the complexes account for their high spin nature.

Antimicrobial assay: Figs. 2 and 3 show the antibacterial and antifungal screening results of free ligands and their Cr(III) complexes, respectively. The findings are compared to those of the standard antibiotics streptomycin and itraconazole, which are used to treat bacteria and fungi, respectively. The findings revealed that newly generated complexes are more biologically active against the same microorganisms than their parent ligands and thier activity increases as concentration increases. When such chemicals are complexed with metal atoms, their biological activity increases significantly. Due to the chelation of metal atoms with the ligand moieties, the metal complexes have a greater inhibitory impact than the parent ligands. Chelation increases the fungicidal activity of a ligand. The positive charge of the metal is partially shared with donor atoms on the ligands and there is electron delocalization over the entire chelate ring, which accounts for the enhanced activity after chelation. As a result, the metal chelate becomes more lipophilic, making it easier for it to pass through the lipid layersof microbial membranes [16]. Furthermore, the chelated complexes are thought to disable a number of cellular enzymes which are important in these microbes' metabolic pathways. Other variables that are altered by the presence of metal ions, such as solubility, conductivity and dipole moment, may further boost the biological activity of metal complexes over ligands.

DNA cleavage activity: Free ligands and their Cr(III) complexes were used in gel electrophoresis assays with *E. coli* (ATCC 25922) DNA. When supercoiled DNA is separated by electrophoresis, DNA with a closed circular confirmation migrates more quickly. At 100 M concentration, the complexes can cause evident plasmid DNA breakage. The metal complexes chosen are capable of converting supercoiled DNA to an open circular shape. DNA cleavage by hydroxyl radicals is explained by generic oxidative mechanisms that involve the removal of a hydrogen atom from sugar units and the release of certain residues from altered sugars depending on the position from where the hydrogen atom is removed. The concentration of the complex, the nature of the metal ion and the presence of
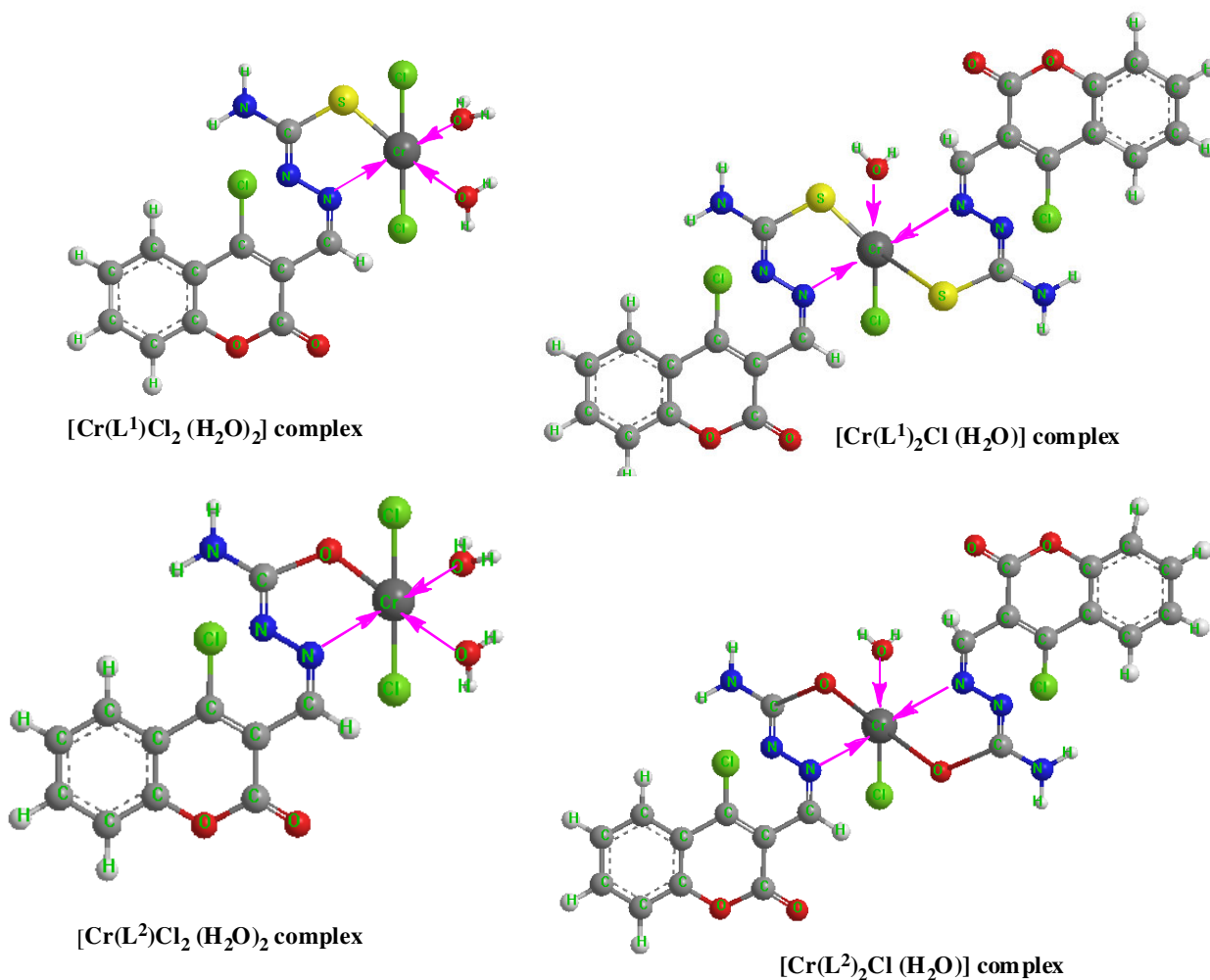
[Cr(L¹)Cl₂ (H₂O)₂] complex

[Cr(L¹)₂Cl (H₂O)] complex

[Cr(L²)Cl₂ (H₂O)₂ complex

[Cr(L²)₂Cl (H₂O)] complex

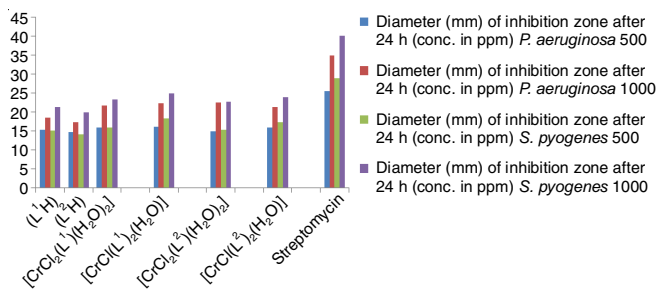Fig. 1. Proposed 3D-structures of the newly obtained metal complexes

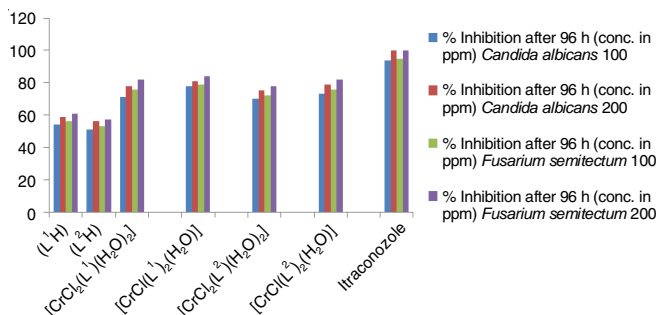Fig. 2. Antibacterial screening data for the ligands (L¹H and L²H) and their chromium(III) complexes

Fig. 3. Antifungal screening data for the ligands (L¹H and L²H) and their chromium(III) complexes

hydrogen peroxide as an exogenous reagent are all important parameters that influence the degree of DNA cleavage by metal complexes [17]. The variable DNA cleavage efficiency of the complexes could be attributable to their different DNA binding affinity. Under comparable experimental settings, complexes display effective DNA cleavage activity in the following order: $[Cr(L^1)_2Cl(H_2O)] > [Cr(L^1)Cl_2(H_2O)_2] > L^1H$ (Fig. 4).
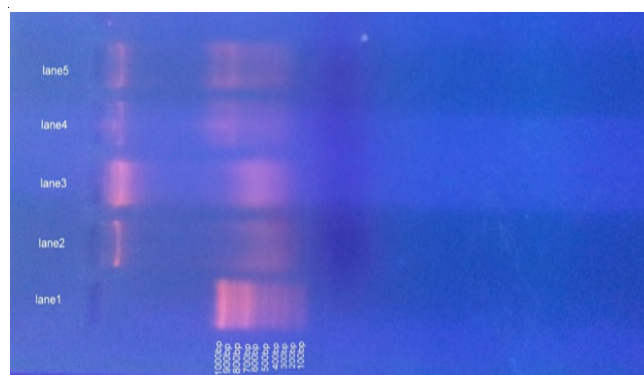

Fig. 4. Lane-1 = DNA Ladder, Lane-2 = uncleaved control *E. coli* Genomic DNA, Lane-3 = cleaved DNA with L¹H, Lane-4 = cleaved DNA with [Cr(L¹)Cl₂ (H₂O)₂], Lane-5 = cleaved DNA with [Cr(L¹)₂Cl (H₂O)]

Conclusion

The synthesis, structural and geometrical characterization and biological features of Cr(III) complexes with nitrogen oxygen/sulphur donor ligands are described. According to spectral and analytical data, the ligands coordinate to the metal atoms in a monobasic bidentate manner, resulting in octahedral geometry. The antimicrobial activity of Cr(III) complexes was found to be greater than that of the ligands. Furthermore, metal complexes have a stronger DNA cleavage activity than parent ligands.

CONFLICT OF INTEREST

The authors declare that there is no conflict of interests regarding the publication of this article.

REFERENCES

1. G.J. Ryan, N.S. Wanko, A.R. Redman and C.B. Cook, *Ann. Pharmacother.*, **37**, 876 (2003);
https://doi.org/10.1345/aph.1C304
2. J.B. Vincent, *Sports Med.*, **33**, 213 (2003);
https://doi.org/10.2165/00007256-200333030-00004
3. A. Çapan, S. Urus and M. Sönmez, *J. Saudi Chem. Soc.*, **22**, 757 (2018);
https://doi.org/10.1016/j.jscs.2017.12.007
4. I.B. Amali, M.P. Kesavan, V. Vijayakumar, R. Rajasekaran, J. Rajesh and G. Rajagopal, *Appl. Biochem. Biotechnol.*, **190**, 373 (2020);
https://doi.org/10.1007/s12010-019-03110-1
5. N. Uddin, F. Rashid, S. Ali, S.A. Tirmizi, I. Ahmad, S.Zaib, M. Zubair, P. L. Diaconescu, M.N. Tahir, J. Iqbal and A. Haider, *J. Biomol. Struct. Dyn.*, **38**, 3246 (2020);
https://doi.org/10.1080/07391102.2019.1654924
6. A.P. King, H.A. Gellineau, J.E. Ahn, S.N. MacMillan and J.J. Wilson, *Inorg. Chem.*, **56**, 6609 (2017);
https://doi.org/10.1021/acs.inorgchem.7b00710
7. T.Y. Fonkui, M.I. Ikhile, P.B. Njobeh and D.T. Ndinteh, *BMC Chem*, **13**, 127 (2019);
https://doi.org/10.1186/s13065-019-0642-3
8. J. Lakshmipraba, S. Arunachalam, R.V. Solomon, P. Venuvanalingam, A. Riyasdeen, R. Dhivya and M.A. Akbarsha, *J. Biomol. Struct. Dyn.*, **33**, 877 (2015);
https://doi.org/10.1080/07391102.2014.918523
9. S. Praveen Kumar, R. Suresh, K. Giribabu, R. Manigandan, S. Munusamy, S. Muthamizh and V. Narayanan, *Spectrochim. Acta A Mol. Biomol. Spectrosc.*, **139**, 431 (2015);
https://doi.org/10.1016/j.saa.2014.12.012
10. S. Alghool, H.F.A. El-Halim and A. Dahshan, *J. Mol. Struct.*, **983**, 32 (2010);
https://doi.org/10.1016/j.molstruc.2010.08.025
11. S.E.A. El-Razek, S.M. El-Gamasy, M. Hassan, M.S. Abdel-Aziz and S.M. Nasr, *J. Mol. Struct.*, **1203**, 127381 (2020);
https://doi.org/10.1016/j.molstruc.2019.127381
12. I. Masih, N. Fahmi and Rajkumar, *J. Enzyme Inhib. Med. Chem.*, **28**, 33 (2013);
https://doi.org/10.3109/14756366.2011.625022
13. P. Kapoor, R.V. Singh and N. Fahmi, *J. Coord. Chem.*, **65**, 262 (2012);
https://doi.org/10.1080/00958972.2011.649265
14. S. Sharma, R. Meena, R.V. Singh and N. Fahmi, *Main Group Met. Chem.*, **39**, 31 (2016);
https://doi.org/10.1515/mgmc-2015-0030
15. N. Fahmi, S. Shrivastava, R. Meena, S.C. Joshi and R.V. Singh, *New J. Chem.*, **37**, 1445 (2013);
https://doi.org/10.1039/c3nj40907d
16. N. Fahmi, A. Kumari, R. Meena and R.V. Singh, *Indian J. Chem.*, **60A**, 341 (2021)
17. J. Viqueira, M.L. Durán, J.A. García-Vázquez, J. Castro, C. Platas-Iglesias, D. Esteban-Gómez, G. Alzuet-Piña, A. Moldes and O.R. Nascimento, *New J. Chem.*, **42**, 15170 (2018);
https://doi.org/10.1039/C8NJ03292K